A Research Report to AFOSR/AOARD

High Temperature Deformation Behavior of Ti-6Al-4V alloy with Widmanstäten Microstructure

by

Jeoung Han Kim and Chong Soo Lee
Center for Advanced Aerospace Materials
Department of Materials Science and Engineering
Pohang University of Science and Technology
Pohang 790-784, KOREA

March 15, 2003

20050111 089

2

REPORT DOCUMENTATION PAGE

1. REPORT DATE *(DD-MM-YYYY)*	2. REPORT TYPE	3. DATES COVERED *(From - To)*
08-09-2004	Final	11-12-2001 to 15-03-2003

4. TITLE AND SUBTITLE

Constitutive analysis on high temperature deformation of Ti-6Al-4V alloy with transformed microstructures

5a. CONTRACT NUMBER
F6256202P0129

5b. GRANT NUMBER

5c. PROGRAM ELEMENT NUMBER

6. AUTHOR(S)

Prof. Chong Soo Lee

5d. PROJECT NUMBER

5e. TASK NUMBER

5f. WORK UNIT NUMBER

7. PERFORMING ORGANIZATION NAME(S) AND ADDRESS(ES)
Pohang University of Science and Technology
San 31, Hyoja-dong, Nam-gu
Pohang 790-784
Korea (South)

8. PERFORMING ORGANIZATION REPORT NUMBER

N/A

9. SPONSORING/MONITORING AGENCY NAME(S) AND ADDRESS(ES)

AOARD
UNIT 45002
APO AP 96337-5002

10. SPONSOR/MONITOR'S ACRONYM(S)

AOARD

11. SPONSOR/MONITOR'S REPORT NUMBER(S)
AOARD-024007

12. DISTRIBUTION/AVAILABILITY STATEMENT

Approved for public release; distribution is unlimited.

13. SUPPLEMENTARY NOTES

14. ABSTRACT

This research established a constitutive model for high-temperature deformation of Ti-6Al-4V alloy with a transformed microstructure. It further investigated the morphological (alpha platelet thickness) effect on the high-temperature plastic flow of transformed microstructure in view of inelastic deformation theory.

15. SUBJECT TERMS

Metals and Alloys, Titanium Alloy, Applied Physics

16. SECURITY CLASSIFICATION OF:			17. LIMITATION OF ABSTRACT	18. NUMBER OF PAGES	19a. NAME OF RESPONSIBLE PERSON
a. REPORT	b. ABSTRACT	c. THIS PAGE			Kenneth C. Goretta, Ph.D.
U	U	U	UU	44	**19b. TELEPHONE NUMBER** *(Include area code)* +81-3-5410-4409

ABSTRACT

A series of load-relaxation tests were conducted on Ti-6Al-4V alloy with a transformed microstructure to investigate high temperature deformation mechanisms. To investigate the effect of lamellar thickness on the high temperature deformation behavior, three transformed microstructures with different α-platelet thickness ($l_\alpha \approx$ 1, 4, and 8 μm, respectively) were produced and tested in this study. The flow stress-vs.-strain rate curves of all three microstructures were well fit with the inelastic deformation equation describing grain matrix deformation (dislocation glide + dislocation climb) at temperatures of 715°C ~ 900°C. However, for the heavily deformed ($\varepsilon \approx$ 1.2) specimens, the operation of grain-boundary sliding was evidenced, which was resulted from the globularization of lamellae. The grain boundary sliding rate (i.e., the globularization) was found to be most rapid for the microstructure with the thinnest alpha laths/platelets. Flow softening of heavily deformed material was attributed to the decrease of σ^* (internal strength variable) due to globularization and the occurrence of grain boundary sliding.

Contents

Chapter 1

Introduction

In the aerospace industry conventional hot working processes such as forging or extrusion are widely used to produce aircraft structural parts. For the production of high quality (homogeneous and defect-free) products, it is necessary to get not only an appropriate design for bulk hot-working process but also clear understanding on the materials behavior at high temperature. As such, active research works have been made on constitutive modeling and analysis for the plastic flow at high temperature, but most of works have neglected the effects of microstructural variation. In addition, most of works have been concentrated on the (single phase) aluminum alloys, and much less work has been carried out for two-phase alloys, such as Ti-6Al-4V alloy. Recently, Semiatin et al. [1-6] conducted extensive works on morphological effects on plastic flow during hot working of Ti-6Al-4V alloy, and provided a general framework for describing constitutive behavior.

Precise description of constitutive behavior is not an easy task due to the fact that an initial microstructure changes with the increase of strain, and texture is also developed during hot working. As an alternative approach, an inelastic deformation theory involving a simple rheological model for grain matrix deformation (GMD), dislocation climb (DC) and grain boundary sliding (GBS) has been proposed by Chang et al. [7] and has been successful in describing overall high temperature deformation behavior of 7475 Al [8], Ti-6Al-4V [9] and gamma-TiAl alloys [10] consisting of equiaxed microstructures.

So far, the inelastic deformation theory has been applied only to the alloys of equiaxed microstructures. It is of great worth to investigate whether the theory is also applicable in the description of high temperature deformation characteristics of transformed microstructures of Ti-6Al-4V. This approach best describes the initial stage of deformation where the peak stress is produced and the amount of deformation is not large. At a later stage of deformation where a large amount of strain ($\varepsilon \approx 1.2$) is imposed, a new mechanism operating at high temperature has been analyzed by inelastic deformation theory and confirmed by optical microscopy. Finally results of this work have been compared and discussed in relation to the earlier works of Semiatin et al. [3].

Therefore, the objectives of this research are to establish a constitutive modeling on high temperature deformation of Ti-6Al-4V alloy with a transformed microstructure, and to investigate the morphological (alpha platelet thickness) effect on the high temperature plastic flow behavior of transformed microstructures in view of inelastic deformation theory.

Manuscript containing some of the results of this work has already been submitted and accepted in the journal of Materials Science Forum, which will be published at July 2003. Another manuscript including most of important results has been written and is going to be submitted to the Acta Materialia. These two papers are included in this final report along with the summary and statement of future work.

Chapter 2

A paper accepted in Materials Science Forum

(July, 2003)

High Temperature Deformation Behavior of Ti-6Al-4V alloy with Widmanstäten Microstructure

Jeoung Han Kim[1], S.L. Semiatin[2] and Chong Soo Lee[1]

[1] Center for Advanced Aerospace Materials
Department of Materials Science and Engineering
Pohang University of Science and Technology, Pohang 790-784, Korea
[2] Air Force Research Lab., Wright-Patterson Air Force Base, OH 45433-7817, USA

Abstract. A series of load-relaxation tests were conducted on Ti-6Al-4V alloy with a transformed microstructure to investigate high temperature deformation mechanisms. The flow stress-vs.-strain rate curves were well fit with the inelastic deformation equation describing grain matrix deformation (dislocation glide + dislocation climb). However, for the heavily deformed ($\varepsilon \approx 1.2$) specimens, the operation of grain-boundary sliding as well as the grain matrix deformation was evidenced. The grain boundary sliding rate was found to be most rapid for the microstructure with the thinnest alpha laths/platelets.

Introduction

High temperature forging is widely applied in the aerospace industry. To produce sound structural parts, it is essential not only to find optimum processing conditions, but also to have clear understanding on the materials behavior at high temperature. So far, active research works have been made on constitutive modeling and analysis for the plastic flow at high temperature, but most of works have not considered the effects of microstructural evolution occurring at high temperature. Furthermore, most of works have been concentrated on the single phase alloys, and much less work has been carried out for two-phase alloys, such as Ti-6Al-4V alloy. Recently, Semiatin et al. [1-5] have conducted extensive works on morphological effects on plastic flow during hot working of Ti-6Al-4V alloy, and provided a general framework for describing constitutive behavior.

However, precise description of constitutive behavior is still required due to the fact that an initial microstructure changes with the increase of strain. As an alternative approach, an inelastic deformation theory involving a simple rheological model for dislocation glide, dislocation climb and grain boundary sliding has been proposed by Chang et al. [6] and has been successful in describing overall high temperature deformation behavior of 7475 Al [7], Ti-6Al-4V [8] and gamma-TiAl alloys [9] consisting of equiaxed microstructures.

This research is aimed to establish a constitutive modeling on high temperature deformation of Ti-6Al-4V alloy with a transformed microstructure, and to investigate the morphological (alpha platelet thickness) effect on the high temperature plastic flow behavior of transformed microstructures in view of inelastic deformation theory.

Inelastic deformation theory

In this model, it is assumed that GBS is mainly accommodated by a dislocation glide process giving rise to an internal strain (a) and non-recoverable plastic stain (α). For the model, the following stress and kinematic relations among the rate variables can be derived:

$$\sigma = \sigma^I + \sigma^F \qquad (1)$$

$$\dot{\varepsilon}_T = \dot{a} + \dot{\alpha} + \dot{g}, \qquad (2)$$

where $\dot{\alpha}$ and $\dot{g}$ denote the plastic strain rates due to dislocation glide and grain-boundary sliding, respectively. The variables σ^I and σ^F are the internal stress due to the long range interaction among dislocations and the friction stress due to the short range interaction between a dislocation and the lattice, respectively. At the high-temperatures used in this study, σ^F is, in general, very small as compared to σ^I, and $\dot{a}$ can be neglected for load-relaxation tests performed under steady-state conditions. Therefore, it is sufficient to describe the constitutive relation at high temperature using the $\dot{\alpha}$, and $\dot{g}$ elements.

The constitutive relation for the plastic strain rate $\dot{\alpha}$ can be formulated as a kinetic equation for the mechanical activation process for the leading-dislocation by the internal stress.

$$(\sigma_\alpha^*/\sigma^I) = \exp(\dot{\alpha}^*/\alpha)^p \qquad (3)$$

$$\dot{\alpha}^* = v^I(\sigma_\alpha^*/G)^{n^I} \exp(-Q_\alpha^I/RT), \qquad (4)$$

where p and n^I are material constants, and σ_α^* and $\dot{\alpha}^*$ denote the internal strength variable and its conjugate reference strain rate, respectively. Equation (4) represents an activation relation for dislocations at grain boundaries, with v^I denoting jump frequency, Q_α^I activation energy, and G an internal modulus. GBS can be represented as stress-induced viscous flow under a frictional drag, thus leading to the following scalar relation between the applied stress and GBS rate

$$(\dot{g}/\dot{g}_0) = [(\sigma - \Sigma_g)/\Sigma_g]^{1/M_g} \qquad (5)$$

$$\dot{g}_0 = v^g(\Sigma_g/\mu^g)^{n^g} \exp(-Q^g/RT), \qquad (6)$$

where M_g is a material constant, and Σ_g and $\dot{g}_0$ are the static friction stress and its conjugate reference rate for GBS, respectively. Equation (6) also represents a thermally activated process of GBS, with Q^g denoting the activation energy for GBS. More detailed description can be found in Refs. [6].

Experimental procedures

A Ti-6Al-4V alloy with (as received) bimodal microstructure was used in this study. To obtain various transformed microstructures, three different heat treatments were given to the specimens; (a) 1040°C/1h + water quenching (b) 1040°C/1h + furnace cooling to room

temp. (c) 1040°C/1h + furnace cooling to room temp. + 976°C/5h + furnace cooling to room temp. In order to get equilibrium microstructures at hot working temperatures, all the samples were heated at 900°C for 2 hours and water quenched. Fig.1 shows the resulting microstructures revealing different lamellar spacings; (a) fine ($\cong$ 1µm), (b) intermediate ($\cong$ 4µm), and (c) coarse ($\cong$ 8µm) lamellar spacing, respectively. All three microstructures had a prior-beta grain size of approximately 300~400 µm.
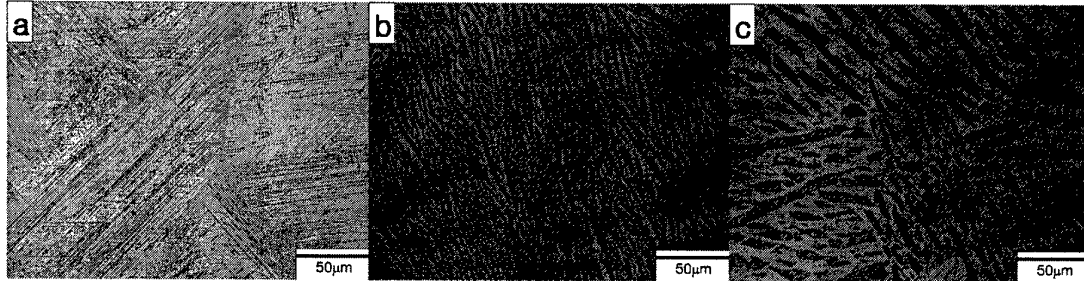

Fig. 1 Optical micrographs showing transformed Ti-6Al-4V alloy with different lamellar spacings; (a) fine ($\cong$ 1µm), (b) intermediate ($\cong$ 4µm), and (c) coarse ($\cong$ 8µm) lamellar spacing microstructures.

Load relaxation tests were used to evaluate the flow stress characteristics of transformed microstructures with different lamellar spacing. The tests was carried out at three different temperatures; 715, 815, and 900°C. During the load relaxation test, microstructure was maintained stable, which was identified by optical microscopy after the test. Round specimens with a gauge diameter of 6.4mm and a gauge length of 27mm was used for the tests. The flow stress and inelastic strain rates obtained by load relaxation tests was analyzed by a non-linear regression method of commercial curve fit program.

Results and discussion

Fig. 2 shows stress-versus-strain-rate curves for the Ti-6Al-4V alloy obtained from the load-relaxation tests at various temperatures. With increasing temperature, the curves shifted toward the region of lower stress and higher strain rate. The effect of lamellar spacing on the flow stress was not consistent, which varied depending on the strain rate. At high strain rate ($\dot{\varepsilon} \geq 10^{-2}$), flow stress increased with decreasing alpha platelet thickness, while the finest lamellar ($l \cong$ 1µm) microstructure revealed lowest flow stress at low strain rate ($\dot{\varepsilon} \leq 10^{-4}$).

The data of 715°C and 815°C were well coincident with the lines drawn based on Equation (3) with an exponent p value of 0.10 (Fig.3). At 900°C, on the other hand, the experimental data shown in Fig. 4 deviated significantly from the lines of Equation (3), especially at the lower strain rate region. This implied that another deformation mode as well as dislocation glide process was also operating at this temperature. Among the various possible deformation modes, the dislocation-climb process was considered to be the most probable to occur at this temperature range [3,9]. The combined curves of dislocation glide and the dislocation-climb process were compared with the experimental data, and a good agreement was observed in Fig. 4.

10

The operation of dislocation-climb process can explain the reverse trend of lamellar spacing effect on flow stress at 900°C. It is noted that all the stress-strain-rate curves obtained in this regime did not reveal any positive curvature, indicating that grain boundary sliding (GBS) did not occur at this conditions.
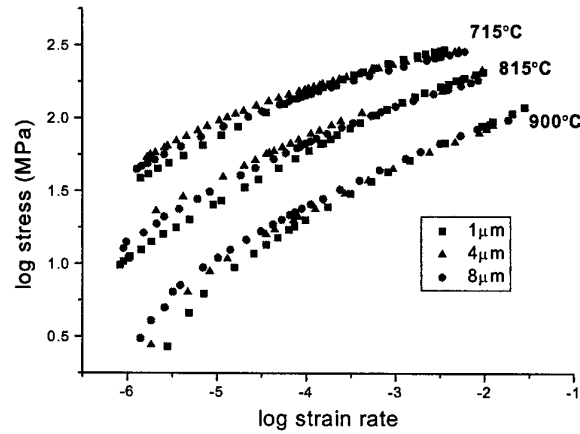

Fig. 2 Stress-strain rate curves of Ti-6Al-4V alloy with a transformed microstructure obtained by load-relaxation tests at various temperatures.
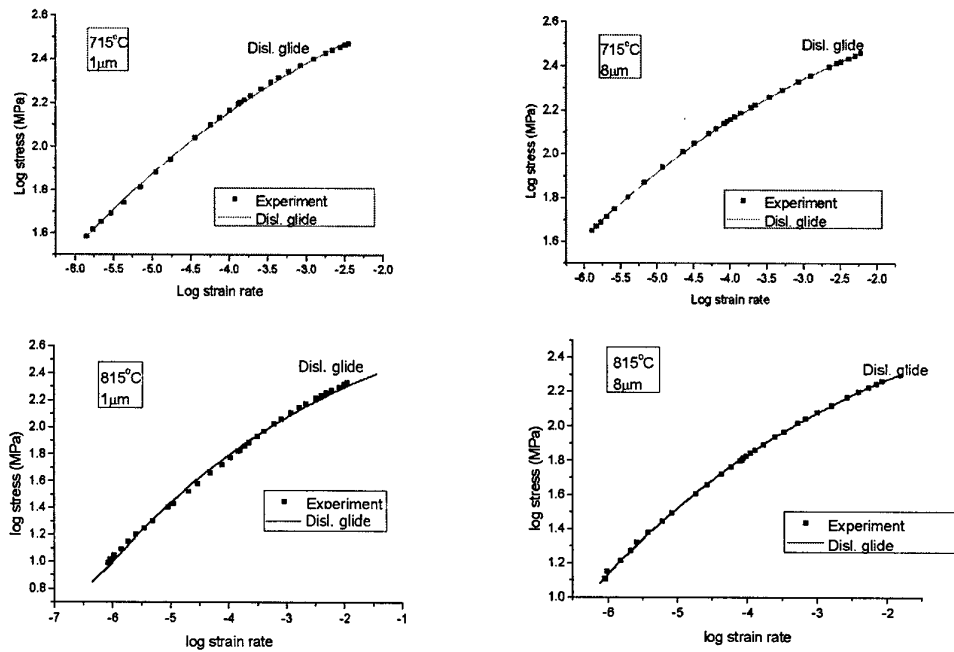

Fig. 3 Experimental flow data (■) and predicted curves of microstructures having various alpha platelet thicknesses ranging from approximately 1 to 8μm at 715 and 815°C.

For the pre-deformed ($\varepsilon \cong 1.2$) specimens, the shape of flow stress curves shown in Fig.5 were analogous to those of the lightly deformed ($\varepsilon \cong 0.05$) specimens. However, the fine
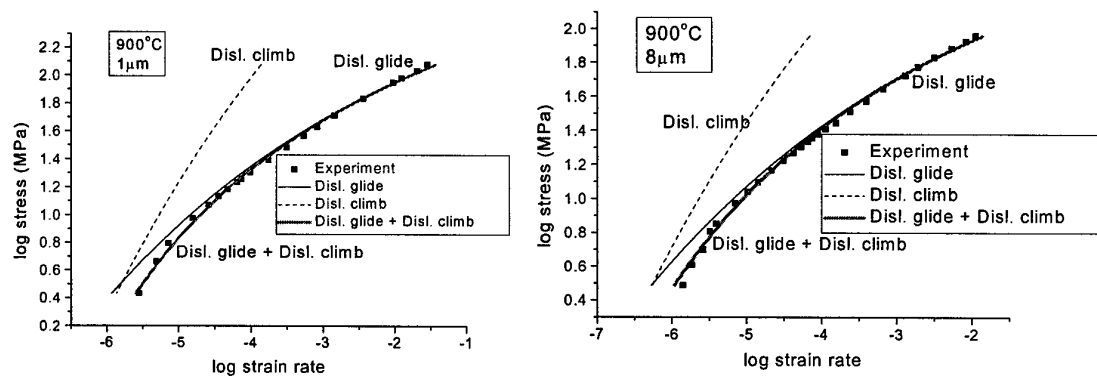
11

Fig. 4 Experimental flow data (■) and predicted curves of microstructures having alpha platelet thicknesses 1μm and 8μm at 900°C.

(1μm) lamellar spacing microstructure revealed the region of positive curvature in the intermediate region of strain rate ($\dot{\varepsilon} = 10^{-5} - 10^{-3}$). According to earlier investigations [8, 9], this curvature change was resulted from the operation of grain-boundary sliding. Consequently, the flow curves of such heavily deformed specimens at 815°C could be drawn by considering two distinctive processes; dislocation glide and grain boundary sliding, which showed good agreement with the experimental data as shown in Fig.5.

It is evident in Fig. 5 that grain boundary sliding rate of "1μm" microstructure is higher than that of "8μm" microstructure at fixed stress level. That is due to the finer equiaxed microstructure produced in the "1μm" lamellar spacing microstructure.
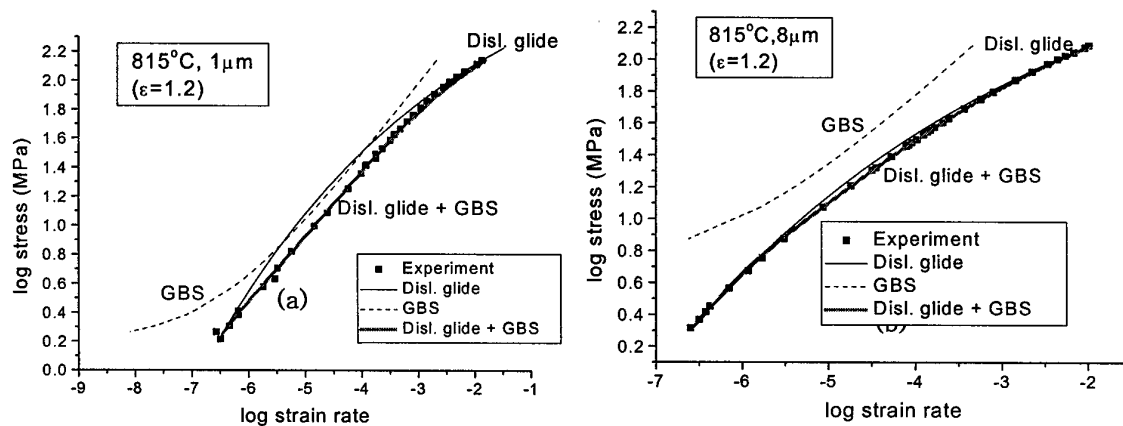
Fig. 5 Experimental data (■) and predicted curves of heavily deformed specimens at 815°C; (a) fine (1μm) and (b) coarse (8μm) lamellar spacing microstructures.

To find the evidences of grain boundary sliding in heavily deformed specimen, pre-deformed "1μm"-specimen was scratched with alumina powder and compressed to ε = 0.2 at 815°C with a strain rate of 10^{-4}/sec. The offset of line (Fig. 6) clearly demonstrates that
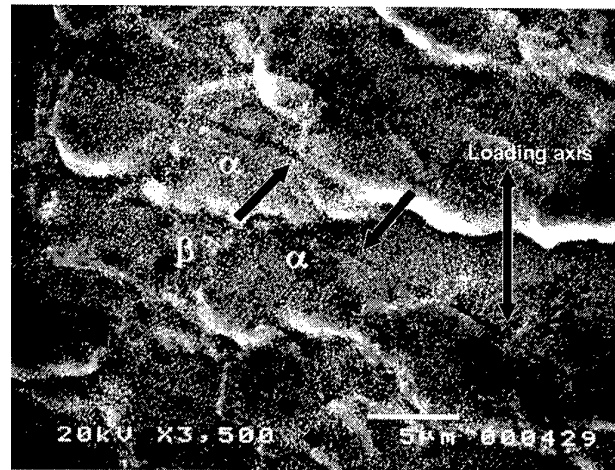
grain boundary sliding took place in the specimen.

Fig. 6 Scratch offset observed at the specimen surface. Specimen was compressed to a strain level of 0.2 (815°C, $\varepsilon \approx 10^{-4}$/sec).

Summary

High temperature deformation mechanisms of Ti-6Al-4V alloy with a transformed microstructure were investigated in view of inelastic deformation theory. The flow stress-strain rate curves obtained by load relaxation tests at 715°C~900°C were well described by the equation for grain matrix deformation. However, for the heavily deformed ($\varepsilon \approx 1.2$) specimen, the flow stress curves changed its shape at the intermediate strain rate region. It was attributed to the operation of grain boundary sliding, the rate of which was highest in the microstructure with the thinnest alpha laths/platelets.

References

[1] S.L. Semiatin and T.R. Bieler, *Metall. Mater. Trans. A*, 2001, 32A, pp. 1787.

[2] S.L. Semiatin and T.R. Bieler, *Acta Mater.*, vol. 49, 2001, pp. 3565.

[3] S.L. Semiatin, V. Seetharaman and I. Weiss, *Materials Science and Engineering A*, vol. A263, 1999. pp. 257-271.

[4] E.B. Shell and S.L. Semiatin, *Metall. Mater. Trans. A*, vol. 30A, 1999, pp. 3219.

[5] S.L. Semiatin, P.A. Kobryn, E.D. Roush, D.U. Furrer, T.E. Howson, R.R. Boyer and D.J. Chellman, *Metall. Mater. Trans. A*, vol. 32A, 2001, pp. 1801.

[6] T.K. Ha and Y.W. Chang, *Acta Mater*, vol. 46, 1998, pp. 2741.

[7] T.K. Ha, Y.N. Kwon and Y.W. Chang, *Mat. Sci. Forum*, vol. 217-222, 1996, pp. 1203.

[8] J.S. Kim, Y.W. Chang and C.S. Lee, *Metall. Trans. A*, vol. 29A, 1998, pp. 217-226

[9] J.H. Kim, D.H. Shin, S.L. Semiatin and C.S. Lee, *Materials Science and Engineering A*. A344, 2003, pp. 146.

Chapter 3

A paper to be submitted to

Acta Materialia

(April, 2003)

Constitutive Analysis on High Temperature Deformation Mechanisms of Ti-6Al-4V alloy with Transformed Microstructure

Jeoung Han Kim, S.L. Semiatin[*] and Chong Soo Lee

Center for Advanced Aerospace Materials

Department of Materials Science and Engineering

Pohang University of Science and Technology, Pohang 790-784, Korea

[*] Air Force Research Lab., Wright-Patterson Air Force Base, OH 45433-7817, USA

Abstract. High temperature deformation mechanisms of Ti-6Al-4V alloy with transformed microstructure were investigated in view of inelastic deformation theory. A series of load-relaxation tests were conducted on three lamellar microstructures with different alpha lamellar spacing at temperatures of 715°C~900°C. The flow stress-vs.-strain rate curves of all microstructures were well fit with the inelastic deformation equation describing grain matrix deformation (dislocation glide + dislocation climb). However, for the heavily deformed ($\varepsilon \approx 1.2$) specimens, the operation of grain-boundary sliding as well as the grain matrix deformation was evidenced. The grain boundary sliding rate was found to be most rapid for the microstructure with the thinnest alpha laths/platelets. Flow softening of heavily deformed material was attributed to the decrease of σ^* (internal strength variable) due to globularization and the occurrence of grain boundary sliding.

1. Introduction

High temperature forging or extrusion is widely applied in the aerospace industry. To produce defect free and homogeneous structural parts, it is essential not only to find optimum processing conditions, but also to have clear understanding on the materials behavior at high temperature. So far, active research works have been made on constitutive modeling and analysis for the plastic flow at high temperature. Especially, the flow behavior of Ti-6Al-4V alloy has received a great interest because of its wide applicability in the industry [1-7]. In primary hot working of Ti-6Al-4V alloy, the conversion of the as-cast large grain microstructure (transformed microstructure) to a fine grain two-phase microstructure (known as globularization in Ti alloys) is an important technological process that leads to a highly formable microstructure suitable for secondary hot working processes such as forging or superplastic forming [8]. The process of breaking down the large grain microstructure to the fine grain microstructure has been a focus of many research efforts [3-6]. Recently, Semiatin et al. investigated the effect of alpha platelet thickness on the plastic flow of Ti-6Al-4V with transformed microstructure by conducting isothermal, hot compression tests. They have suggested that deformation is controlled by a dislocation glide-climb mechanism characteristic of power-law creep, and peak flow stress which characterizes the low strain plastic flow behavior of the transformed microstructures follow a Hall-Petch dependence on alpha lath/platelet thickness. However, earlier approaches have not considered the effects of microstructural evolution occurring at high temperature before or during the processing. Furthermore, precise description of constitutive behavior can not be well defined in this manner.

Another approach has been made to establish constitutive equations based on dislocation dynamics. Recently, the constitutive equations on the basis of inelastic deformation theory

has been proposed by Chang et al. [9], and successful in describing overall high temperature deformation behavior of Al alloys [10], Ti-6Al-4V [11] and γ-TiAl alloys [12] consisting of equiaxed microstructures.

This research is aimed to establish a constitutive modeling on high temperature deformation of Ti-6Al-4V alloy with a transformed microstructure, and to investigate the morphological (alpha platelet thickness) effect on the high temperature plastic flow behavior of transformed microstructures in view of inelastic deformation theory.

2. Internal variable theory of inelastic deformation

Fig.1 shows a rheological and a topological model for inelastic deformation, including grain matrix deformation (GMD) and grain-boundary sliding (GBS). The former comprises plastic deformations due to a dislocation glide process giving rise to an internal strain (a) and non-recoverable plastic stain (α), and dislocation climb process (β). For the model shown in Fig.1, the following stress and kinematic relations among the rate variables can be derived:

$$\sigma = \sigma^I + \sigma^F \quad \text{--(1)}$$

$$\dot{\varepsilon}_T = \dot{a} + \dot{\alpha} + \dot{\beta} + \dot{g}, \quad \text{-------------------------------(2)}$$

where $\dot{\alpha}$, $\dot{\beta}$, and $\dot{g}$ denote the plastic strain rates due to dislocation glide, dislocation climb, and grain-boundary sliding, respectively. The variables σ^I and σ^F are the internal stress due to the long range interaction among dislocations and the friction stress due to the short range interaction between a dislocation and the lattice, respectively. At the high-

temperatures used in this study, σ^F is, in general, very small as compared to σ^I, and the internal strain rate $\dot{\alpha}$ can be neglected for load-relaxation tests performed under steady-state conditions. Therefore, it is sufficient to describe the constitutive relation at high temperature using the $\dot{\alpha}$, $\dot{\beta}$ and $\dot{g}$ elements (Fig.1).

The constitutive relation for the plastic strain rate $\dot{\alpha}$ can be formulated as a kinetic equation for the mechanical activation process of the leading-dislocation by the internal stress. For uniaxial tension, the scalar relation is expressed in a form similar to that of Hart [16], i.e.,

$$(\sigma_\alpha{}^*/\sigma^I) = \exp(\dot{\alpha}{}^*/\alpha)^p \quad \text{------------------------------------(3)}$$

$$\dot{\alpha}{}^* = \nu^I(\sigma_\alpha{}^*/G)^{n^I} \exp(-Q_\alpha{}^I/RT), \quad \text{----------------------(4)}$$

where p and n^I are material constants, and $\sigma_\alpha{}^*$ and $\dot{\alpha}{}^*$ denote the internal strength variable and its conjugate reference strain rate, respectively. Equation (4) represents an activation relation for dislocations at grain boundaries, with ν^I denoting jump frequency, $Q_\alpha{}^I$ activation energy, and G an internal modulus.

Grain boundary sliding can be represented as stress-induced viscous flow under a frictional drag, thus the following scalar relation between the applied stress and GBS rate can be derived;

$$(\dot{g}/\dot{g}_o) = [(\sigma - \Sigma_g)/\Sigma_g]^{1/M_g} \quad \text{---------------------------------(5)}$$

$$\dot{g}_o = \nu^g(\Sigma_g/\mu^g)^{n^g} \exp(-Q^g/RT), \quad \text{--------------------------(6)}$$

where M_g and n^g are material constants, and Σ_g and $\dot{g}_o$ are the static friction stress and its

conjugate reference rate for GBS, respectively. Equation (6) also represents a thermally activated process of GBS, with Q^g denoting the activation energy for GBS.

Like the plastic strain rate $\dot{\alpha}$, the strain rate due to the dislocation-climb process, $\dot{\beta}$, can be formulated as follows [15].

$$(\sigma_\beta^*/\sigma^I) = \exp(\dot{\beta}^*/\dot{\beta})^p \text{ --(7)}$$

$$\dot{\beta}^* = \nu^I(\sigma_\beta^*/G)^{n^I} \exp(-Q_\beta^I/RT) . \text{ ------------------------(8)}$$

3. Experimental procedures

Ti-6Al-4V alloy used in this study was provided by TIMET with a hot-rolled plate (t ≈ 40 mm). As-received plate revealed a bimodal microstructure as shown in Fig. 2. The chemical composition of the alloy was 6.19 Al, 4.19 V, 0.29 Fe, 0.17 O, 0.016 C, 0.004 N, and 0.007 H in weight percent with the balance titanium.
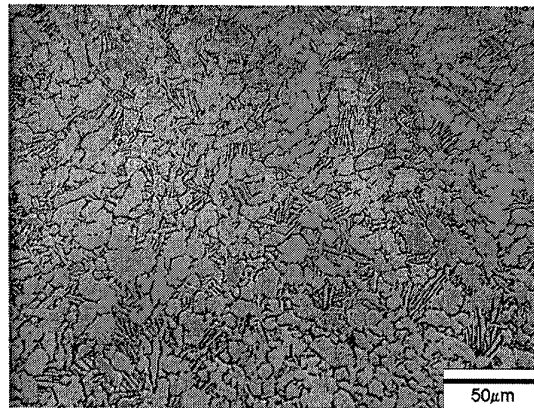

Fig. 2. Optical micrograph of as-received Ti-6Al-4V alloy used in this study.

To obtain various transformed microstructures, three different heat treatments were given to the specimens; (a) 1040°C/1h + water quenching (b) 1040°C/1h + furnace cooling to room temp. (c) 1040°C/1h + furnace cooling to room temp. + 976°C/5h + furnace cooling to room temp. In order to get equilibrium microstructures at hot working temperatures, all the samples were heated at 900°C for 2 hours and water quenched. Fig. 3 shows the resulting microstructures revealing different lamellar spacings; (a) fine ($\cong$ 1μm), (b) intermediate ($\cong$ 4μm), and (c) coarse ($\cong$ 8μm) lamellar microstructures, respectively. All three microstructures had a prior-beta grain size of approximately 300~400 μm.

Load relaxation tests were used to evaluate the flow stress characteristics of transformed microstructures with different lamellar spacing. The test was carried out at three different temperatures; 715, 815, and 900°C using round specimens with a gauge diameter of 6.4mm and a gauge length of 27mm. During the load relaxation test, microstructure was maintained stable, which was identified by optical microscopy after the test. To minimize oxidation, gauge section of all the specimen was coated with a glass lubricant before being placed in the test machine. To investigate the flow behavior of the material after imposing a large amount of deformation, load-relaxation test was also conducted on heavily deformed specimens ($\varepsilon \cong 1.2$). For all load-relaxation experiments, the load-time (P-t) curves were converted to flow stress versus strain rate (σ-$\dot{\varepsilon}$) curves by applying the methods proposed by Lee and Hart [16]. As evidenced by microstructural analysis, the microstructures were not significantly changed before or during the load-relaxation test. The flow stress - inelastic strain rates curves obtained by load relaxation test were analyzed by a non-linear regression method of commercial curve fit program.
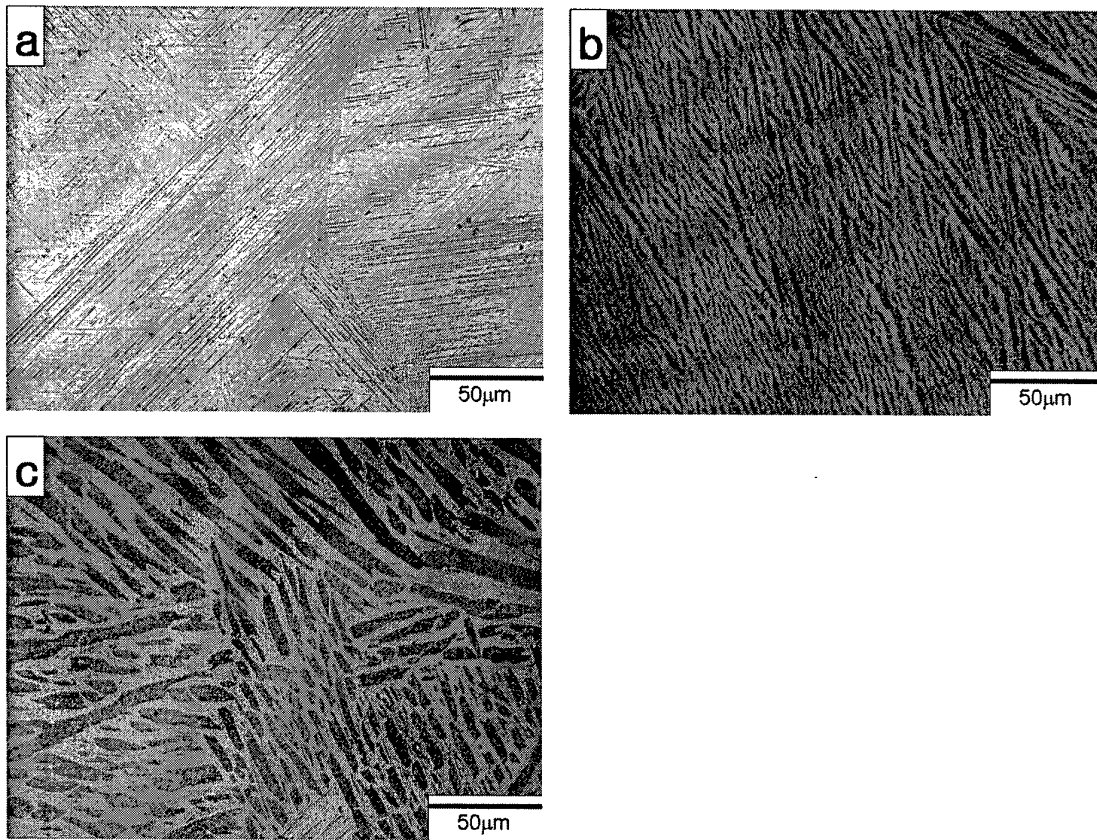
Fig. 3 Optical micrographs showing transformed Ti-6Al-4V alloy with different lamellar spacings; (a) fine ($\cong 1\mu m$), (b) intermediate ($\cong 4\mu m$), and (c) coarse ($\cong 8\mu m$) lamellar spacing microstructures.

To confirm the results of the load-relaxation test, tension tests were conducted using flat specimens with gauge dimensions of 10 mm length, 5 mm width, and 2 mm thickness on an automated static test machine (Instron 1361) equipped with a three-heating-zone furnace. Tension tests were performed at room temperature and 815°C and initial strain rates of 1×10^{-1} and 1×10^{-4}/sec. After tension testing, each specimen was water quenched and examined by optical microscopy.

4. Results

4.1 Load-relaxation tests at a strain level of 0.05

Fig. 4 shows stress-versus-strain-rate curves for the Ti-6Al-4V alloy obtained from the load-relaxation tests at various temperatures. With increasing temperature, the curves shifted toward the region of lower stress and higher strain rate. The effect of lamellar spacing on the flow stress was not consistent, which varied depending on the strain rate. At high strain rate ($\dot{\varepsilon} \geq 10^{-2}$), flow stress increased with decreasing alpha platelet thickness, while the finest lamellar ($l \cong 1\mu m$) microstructure revealed lowest flow stress at low strain rate ($\dot{\varepsilon} \leq 10^{-4}$). Similar trend of data has also been reported in the work of Semiatin et al. [7] performed by compression test. This indicates that flow stress is sensitively varied not only by the strain rate but also by the lamellar spacing. It is likely that deformation mechanism operating at low strain rate is different from that of the higher strain rate.
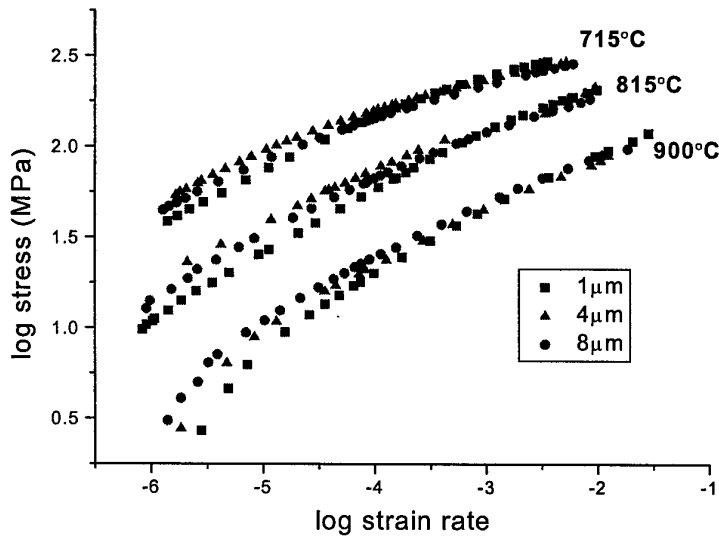

Fig. 4 Stress-strain rate curves of Ti-6Al-4V alloy with a transformed microstructure obtained by load-relaxation tests at various temperatures.

Fig.5 shows that the flow stress data of 715°C and 815°C are well coincident with the solid lines drawn based on Equation (3) describing dislocation glide. The solid lines are the fits of Equation (3) using the constitutive parameters obtained by non-liner regression method. Here, it is noted that all the data were well fit when using an exponent p of 0.10, which is different from the earlier works [12,13,15]. The constitutive parameters ($\sigma_\alpha^*, \dot{\alpha}^*$, and p) for dislocation glide are summarized in Table I.
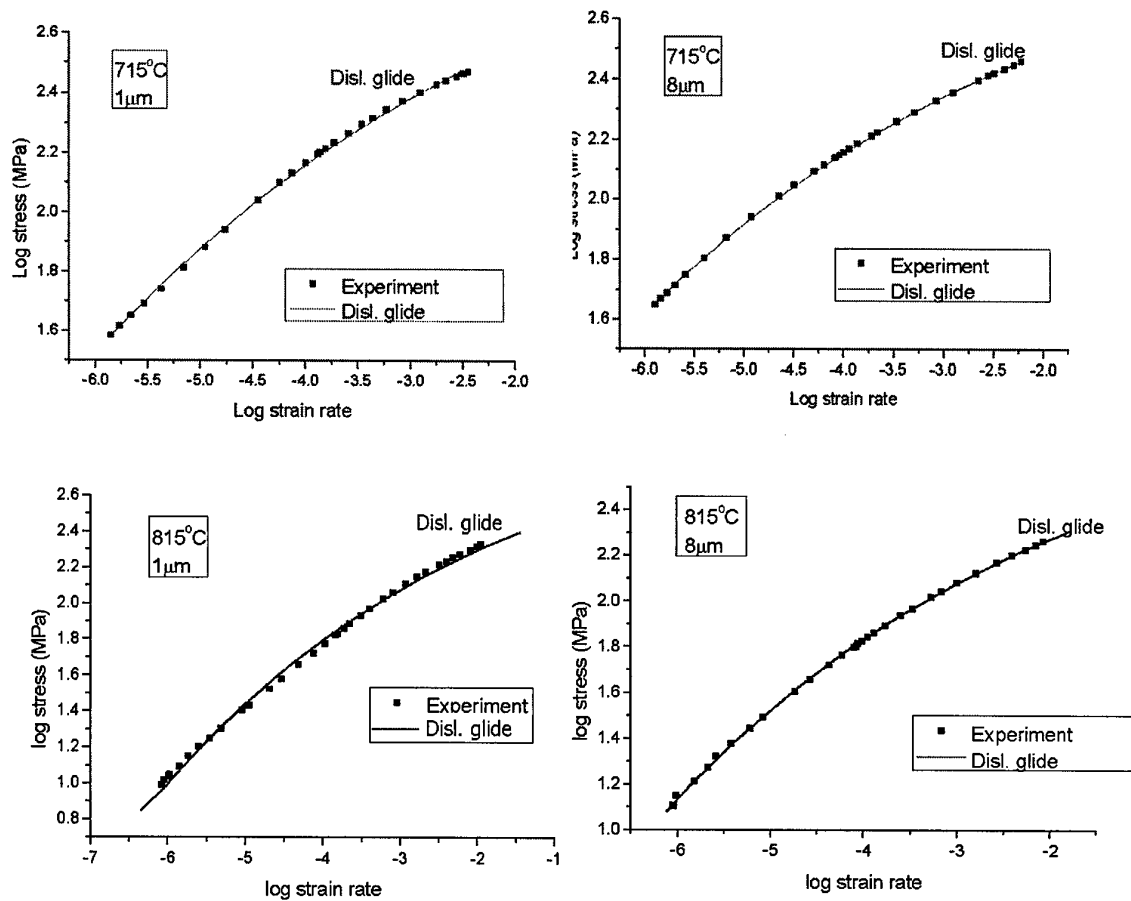

Fig. 5 Experimental flow stress and strain rate data (■) and predicted curves using Equation (3) for microstructures with alpha platelet thickness of (a,c) 1 μm and (b,d) 8μm tested at (a,b) 715 and (c,d) 815°C.

At 900°C, on the other hand, the experimental data shown in Fig. 6 deviated significantly from the lines of Equation (3), especially at the lower strain rate region. It was considered that an additional deformation mode other than dislocation glide process might operate at this temperature and strain rate region. Among the various possible deformation modes, the dislocation-climb process was considered to be the most probable for the additional deformation mechanism at this high temperature and low strain rate as discussed later in Section 5.1. The grain boundary sliding rate ($\dot{g}$) was assumed to be zero because the stress-strain rate curves obtained in this regime did not reveal the concave shape characteristic of the GBS mode [12-15]. Besides, microstructural observation did not show any trace of the GBS. By considering dislocation glide and dislocation climb, excellent fits to the experimental data were obtained. For this purpose, the values of strain rate for the dislocation climb process ($\dot{\beta}$) were estimated from Equation (7). These values were subsequently used for a non-linear curve fitting of Equation (7) to determine the constitutive parameters (σ_β^*, β^*, and p) for the dislocation climb process.
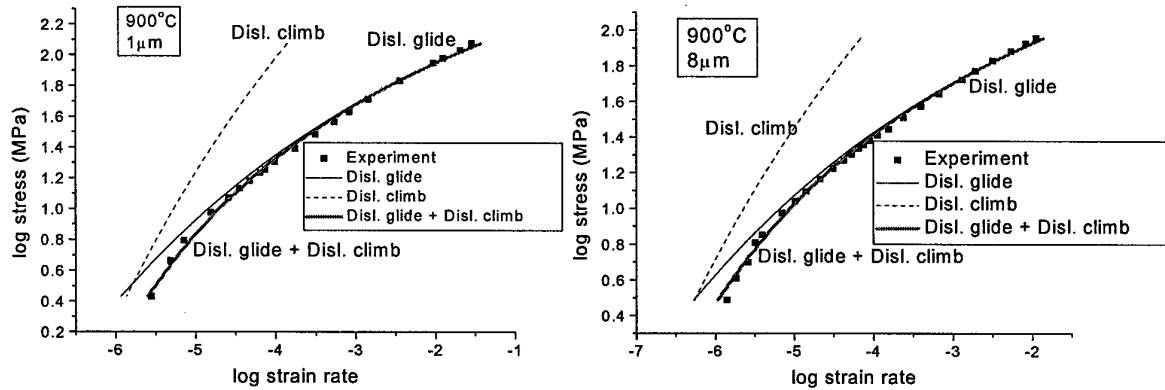

Fig. 6 Experimental flow stress and strain rate data (■) and predicted curves using Equations (3) and (7) for microstructures having alpha platelet thicknesses of 1μm and 8μm tested at 900°C.

The dotted lines in Fig. 6 represent the predicted curves for the dislocation climb process. The combined curves of dislocation glide and the dislocation-climb process were compared with the experimental data, and a good agreement was observed. The operation of dislocation-climb process can explain the reverse trend of lamellar spacing effect on flow stress at 900°C. The constitutive parameters for dislocation climb, as well as dislocation glide, are also summarized in Table I. It is noted that the parameter p characterizing the dislocation permeability of strong barriers was determined to be 0.10, which is different from that in other FCC and BCC materials [12,13,15].

Table I. The constitutive parameters determined from load-relaxation tests at a strain of 0.05.

Temp.	Micro-structure	Dislocation slip			Dislocation climb		
		$\log \sigma_\alpha{}^*$	$\log \dot{\alpha}{}^*$	p	$\log \sigma_\beta{}^*$	$\log \dot{\beta}{}^*$	p
715°C	1μm	3.24	-0.03	0.1	-	-	-
	4μm	3.03	-1.11	0.1	-	-	-
	8μm	3.06	-0.78	0.1	-	-	-
815°C	1μm	3.22	1.15	0.1	-	-	-
	4μm	3.08	0.42	0.1	-	-	-
	8μm	3.04	0.41	0.1	-	-	-
900°C	1μm	2.98	1.75	0.1	4.87	4.22	0.1
	4μm	2.81	1.15	0.1	4.61	3.81	0.1
	8μm	2.79	0.97	0.1	4.36	3.17	0.1

4.2 Load-relaxation tests at a strain level of 1.2

To investigate the effect of strain amounts on the flow behavior of Ti-6Al-4V alloy, all three samples with different lamellar spacing were hot rolled to a strain level of 1.2 at

900°C and quenched. Fig. 7 shows resulting microstructures after heavy deformation was imposed. As shown in Fig. 7, for a given amount of deformation, thin alpha lamella material is more easily converted into an equiaxed morphology than is thick lamella material, which has also been reported in elsewhere [6,17]. It is clear that the morphology change (from high aspect ratio into low aspect ratio of alpha lamellae) has been resulted from a break up of the alpha lamellae. In Fig.7-(c), on the other hand, there are some fine equiaxed grains of which diameter is much smaller than the thickness of alpha plate. It shows that dynamic recrystallization of alpha grain took place in thick lamella material, as indicated by arrows in the Fig. 7-(c).
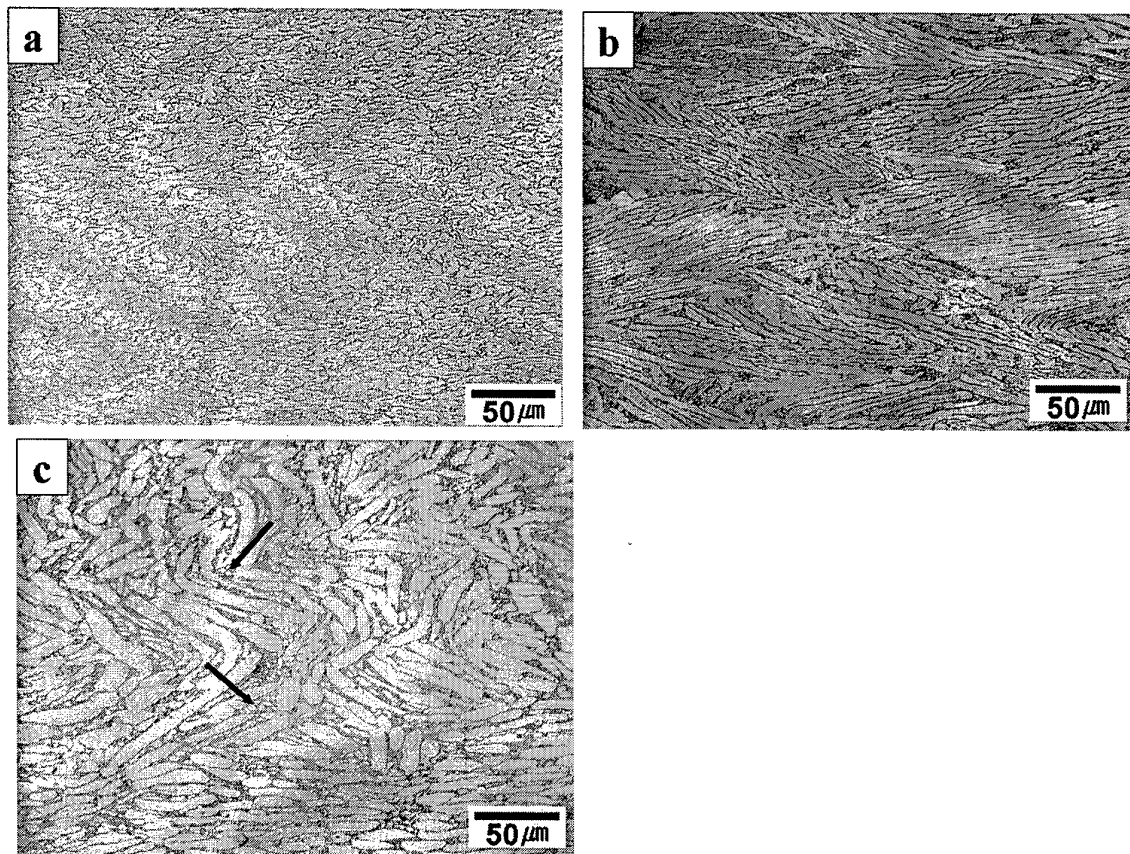

Fig. 7. Optical micrographs showing the microstructures of hot rolled Ti-6Al-4V alloy which had initial lamellar spacings of; (a) 1μm, (b) 4μm, and (c) 8μm.

Fig. 8 shows aspect ratios of three materials after hot rolling, and the change of the aspect ratios before and after the deformation is shown in Table II. Here, the globularization ratio was obtained by considering the aspect ratios before and after the deformation.
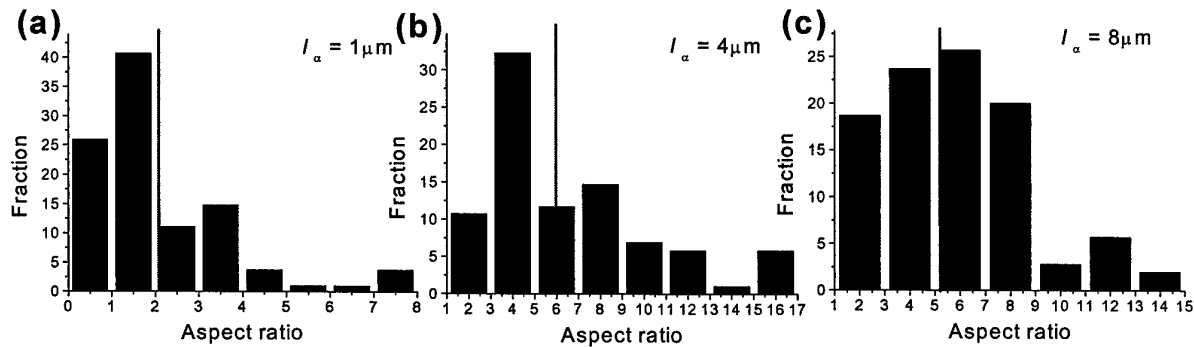

Fig. 8. Charts showing aspect ratios of hot rolled Ti-6Al-4V alloy which had initial lamellar spacings of; (a) 1μm, (b) 4μm and (c) 8μm.

Table II. The changes in the aspect ratio of three materials before and after hot rolling.

Thickness	Before rolling	After rolling	Globularization ratio
$l_\alpha \cong 1\ \mu m$	20~30	2.06	~15.0
$l_\alpha \cong 4\ \mu m$	~10	5.91	~1.7
$l_\alpha \cong 8\ \mu m$	~6	5.20	~1.2

Using the heavily deformed materials ($\varepsilon \cong 1.2$), additional load-relaxation test was conducted at 815 and 900°C and the results are given in Fig. 9 and Table III. The flow stress-strain rate curves of the microstructure with thick alpha plate (Fig.9b and 9d) was analogous to those of the lightly deformed ($\varepsilon \cong 0.05$) specimens. However, the fine (1μm) lamellar spacing microstructure revealed the region of positive curvature at the region of

intermediate strain rate ($\dot{\varepsilon} = 10^{-5} \sim 10^{-3}$). The appearance of the concave portion in the curves implies that the grain-boundary sliding operates along with the dislocation glide and climb [12].

Table III. The constitutive parameters determined from load-relaxation tests at a strain level of 1.2.

Temp.	Micro-structure	Dislocation slip			Grain boundary sliding		
		$\log \sigma_\alpha^*$	$\log \sigma_\alpha^*$	p	$\log \varepsilon_o$	$\log \Sigma_o$	M_g
815°C	1μm	3.14	1.78	0.1	-6.56	0.196	0.5
	4μm	3.04	1.51	0.1	-6.15	0.621	0.5
	8μm	3.02	1.38	0.1	-6.12	0.680	0.5
900°C	1μm	2.85	2.04	0.1	-6.44	-0.506	0.5
	4μm	2.75	1.62	0.1	-5.85	0.255	0.5
	8μm	2.71	1.51	0.1	-5.91	0.269	0.5

Consequently, the flow stress-strain rate curves of such heavily deformed specimens at 815°C could be drawn by considering two distinctive processes; dislocation glide and grain boundary sliding, which showed good agreement with the experimental data as shown in Fig.9a and 9b. The flow stress-strain rate curves of 900°C represented additional deformation mechanism i.e dislocation climb but its contribution to total deformation was considered negligible.

It is evident in Fig.9 that grain boundary sliding rate of "1μm" microstructure is higher than that of "8μm" microstructure at fixed stress level. That is due to the finer equiaxed microstructure produced in the "1μm" lamellar spacing microstructure after heavy deformation.

4.3 Tensile tests

To examine the results of the load-relaxation test, tension tests were conducted at room and high temperatures. Fig. 10 shows the macrographs of fractured tensile specimens at 815°C (Fig. 10-a,b) and room temperature (Fig. 10-c).

In Fig.10-(a), the "1μm alpha plate" specimen tested at strain rate of 10^{-1}/sec showed ductile fracture while the others (4 and 8 μm) fractured making an angle of approximately 45° with the tensile axis, indicating a brittle fracture phenomenon.

At low strain rate of 10^{-4}/sec, all the specimens showed relatively large elongation at 815°C. Especially, "1μm alpha plate" exhibited superplastic deformation behavior elongated to a strain of 2.7. The reason of this large elongation, in spite of high aspect ratio of initial microstructure, was attributed to occurrence of the dynamic globularization during the tensile test. Meanwhile, at room temperature, all the specimens show nature of brittle fracture.

5. Discussion

5.1 Deformation mechanisms in view of internal variable theory of inelastic deformation

The experimental results have shown that that dislocation glide, grain boundary sliding, dislocation climb, and dynamic globularization contribute in varying degrees to the total deformation of Ti-6Al-4V alloy with a transformed microstructure. In the early stages ofdeformation, flow behavior is mainly governed by dislocation glide. At high temperature (above 815°C), additional deformation mechanism appears at low strain rate region. Identical behavior was also observed in Ti-Al, Fe-23Al, and β-CuZn [15, 18, 19]. Fig.11 shows TEM micrographs showing sub-boundary with SADP, and magnified microstructure
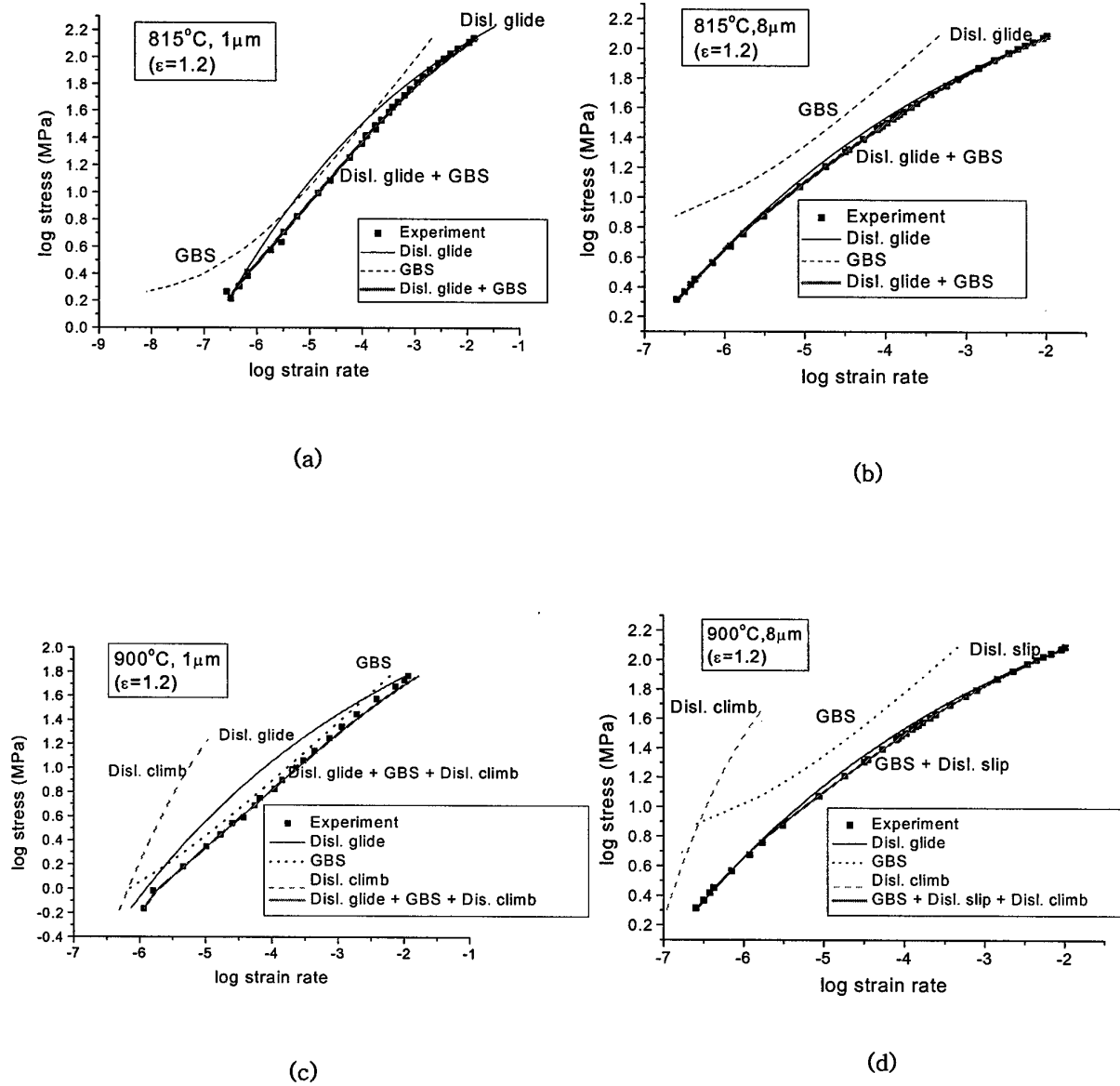
(a)

(b)

(c)

(d)

Fig. 9 Experimental flow stress – strain rate data (■) and predicted curves of heavily

deformed specimens; (a) 1μm, 815°C, (b) 8μm, 815°C,   900°C; (c) 1μm, 900°C and
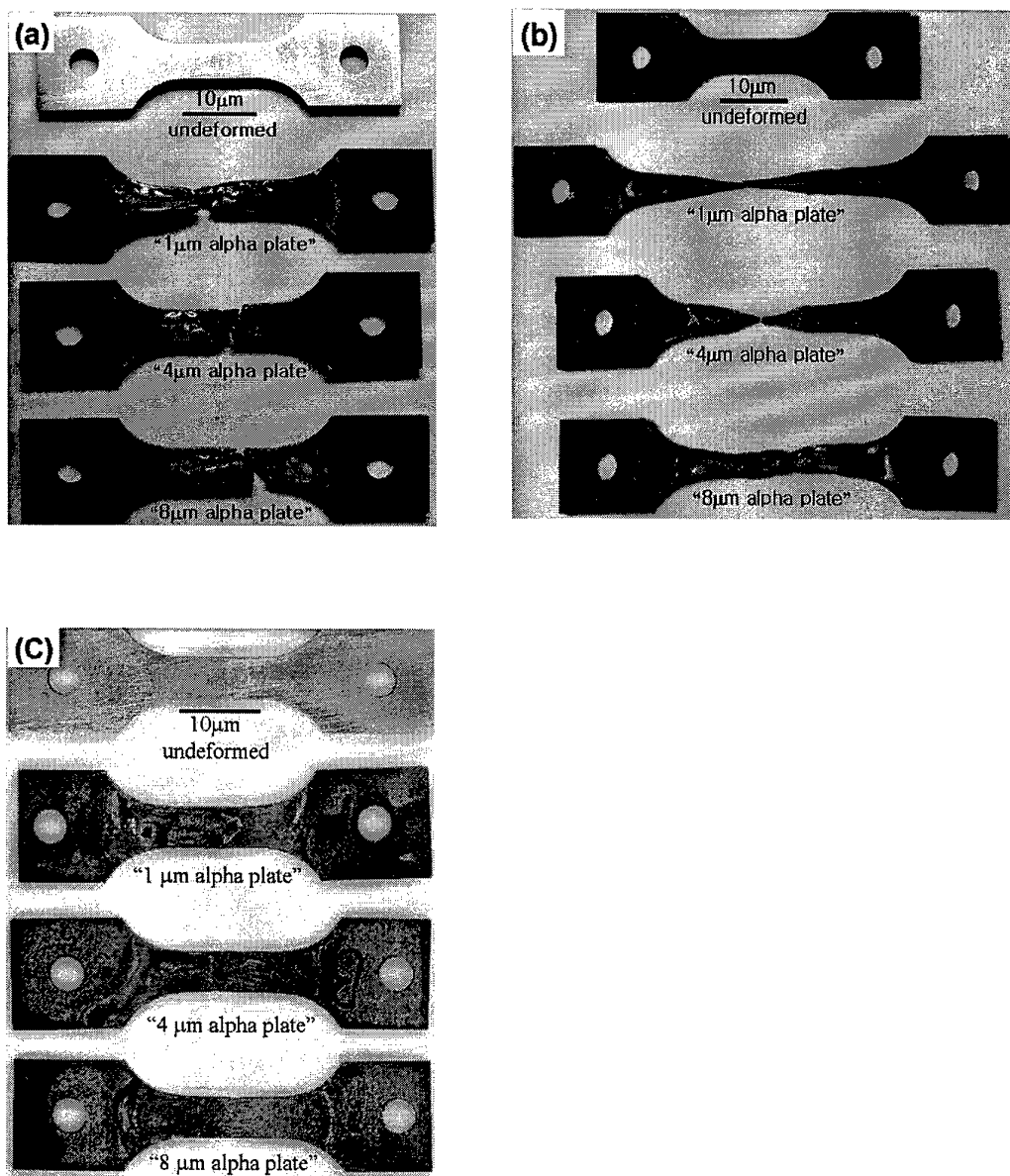
(d) 8μm, 900°C.

Fig.10 Macrographs of fractured tensile specimens tested at 815°C using initial strain rate of; (a) 10^{-1}/sec and (b) 10^{-4}/sec; and (c) at room temperature, 10^{-4}/sec.

with g=(110) in Fe-23Al deformed at 600°C [18]. In Fig 11(a), region (1) and region (2) reveal same diffraction pattern indicating that two regions are located in the same one grain. Fig.11(b) reveals that the sub-boundary is composed of many dislocation net-works. Dislocation climb can occur readily at high temperature and the dislocations arrange themselves into a low-angle grain boundary. Considering the result of Fe-23Al, it is suggested that the additional mechanism operating at 900°C in this study has been resulted from dislocation climb.
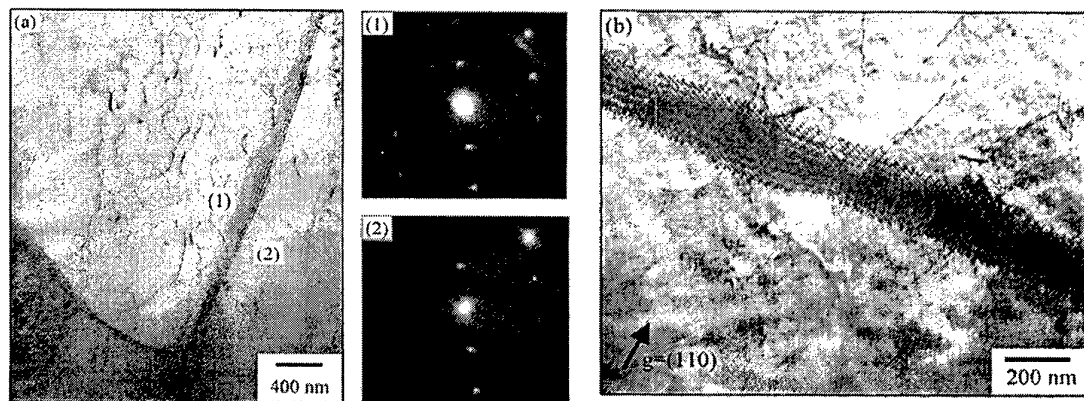

Fig.11 TEM micrographs showing sub-boundaries with (a) SADP, and (b) magnified view with g=(110) in Fe-23Al deformed at 600°C [18].

Evidence of grain-boundary sliding was not observed at this test condition in either optical micrographs or the load-relaxation tests. It is natural considering the high aspect ratio of un-deformed materials.

However, at high strain level of 1.2, dynamic globularization started to occur and alpha lamellae became more equiaxed ones. After the large amounts of deformation, the constitutive behavior of the Ti-6Al-4V alloy was controlled by both dislocation glide and grain boundary sliding, while the dislocation climb process did not seem to play a significant role. For the thinnest alpha plate material, grain-boundary sliding contributed

noticeably to the total deformation since the dynamic globularization was most efficient in this material resulting in the significant grain refinement.

To find the evidences of grain boundary sliding in heavily deformed specimen, pre-deformed "1μm"-specimen was scratched with alumina powder and compressed to $\varepsilon = 0.2$. The test was carried out at 815°C with a strain rate of 10^{-4}/sec where the operation of grain-boundary sliding is expected. In Fig.12, the offset of a line was detected at α/α boundary which clearly demonstrates that grain boundary sliding took place in the specimen. The offset can be produced by grain rotation mechanism as well as grain boundary sliding [20]. In that case, the offseted-scratch lines should not be parallel and misfit boundaries must be shown separately at two different places. However, this phenomenon is not shown in Fig.12. It is noted that the scratch line in grain interior is relatively sharp and straight, which implies that grain matrix deformation is not significant.
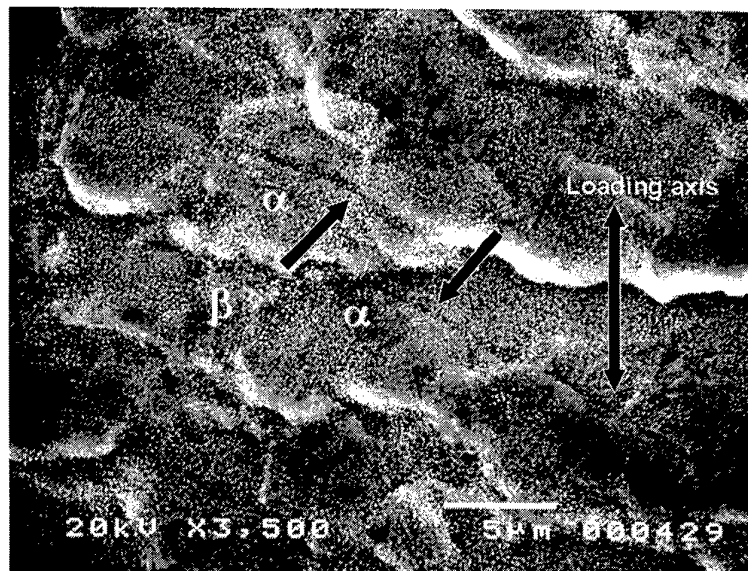

Fig. 12 Scratch offset observed at the specimen surface. Specimen was compressed to a strain level of 0.2 (815°C, $\dot{\varepsilon} \approx 10^{-4}$/sec).

33

5.2 Flow softening behavior

Fig. 13 shows the flow stress versus strain rate curves of "1μm" material obtained at a strain level of 0.05 and 1.2, respectively. The flow stress of lightly deformed specimen is much lower than that of heavily deformed specimen through the entire strain rate region. It is evident in Fig. 13 that flow softening of heavily deformed specimen is resulted from (1) the ease of dislocation glide (i.e., the shift of dislocation glide line to lower stress region) due to globularization and (2) the occurrence of grain boundary sliding.

It is obvious that the occurrence of grain boundary sliding can lower the flow stress at the region of intermediate strain rate ($\dot{\varepsilon} = 10^{-5} - 10^{-3}$). But the reason of the easiness of dislocation glide in the globularized microstructure is not clear. One possible reason is that this behavior is closely related to increase of grain boundary area above equi-cohesive temperature. Total flow strength can be explained by the sum of grain interior strength and grain boundary strength. As the dynamic globularization process proceeds, alpha platelet breaks up and then, total area of grain boundary increases. Above equi-cohesive temperature, the strength of grain boundary is lower than that of grain interior. Thus, opposite behavior to the Hall-Petch relationship between strength and grain size should appear at this condition [20,21]. The temperature of 815°C is obviously over the equi-cohesive temperature according to the previous work [14]. Thus, it is suggested that the increase of grain boundary area due to dynamic globularization results in the loss of total flow strength at this temperature.

The decrement of σ^* value with the increase of strain from 0.05 to 1.2 are presented in Table IV. Degree of softening at strain rate of 10^{-1}/sec is largest in the finest lamellar microstructure which has the largest grain boundary area due to globularization. The

decrement of σ^* value implying internal strength is also largest in this finest lamellar microstructure. It appears that ratio of the σ^* decrement with the alpha platelet thickness is similar to that of softening at strain rate of 10^{-1}/sec.
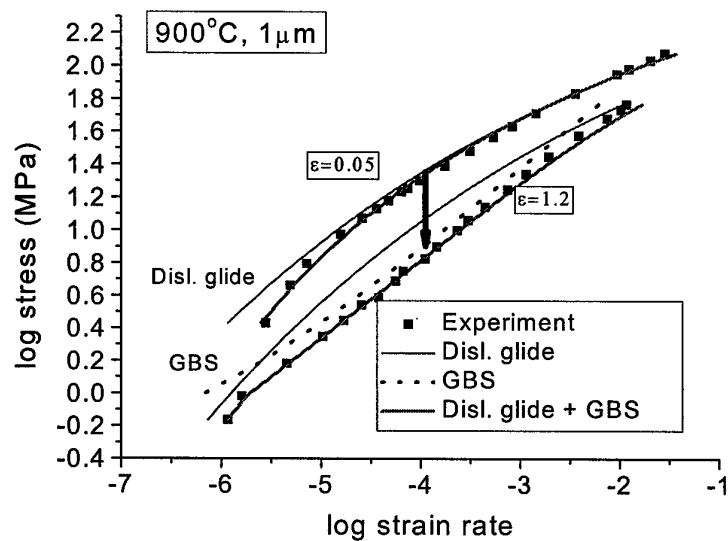

Fig. 13 Flow stress decreases after hot deformation due to dynamic globularization.

Table IV. The decrement of internal strength variable and flow stress at a strain rate of 10^{-1}/sec with the increase of strain from 0.05 to 1.2.

Temp.	Micro-structure	$\Delta \log \sigma^*$	Δ flow stress at 10^{-1}/sec
815°C	1μm	0.08	114 MPa
	4μm	0.04	98 MPa
	8μm	0.02	84 MPa
900°C	1μm	0.13	51 MPa
	4μm	0.06	36 MPa
	8μm	0.08	41 MPa

5.3. Changes in the order of flow stress at low strain rate

Fig.14 shows flow stress-strain curves obtained at 815°C and room temperature using initial strain rate of 10^{-1}/sec and 10^{-4}/sec. In Fig.14(a) and Fig.14(b), all of the stress-strain curves obtained at 815°C exhibited a peak stress at low strains and a noticeable flow softening irrespective of test strain rate and microstructure.

At the strain rate of 10^{-1}/sec, the peak stress increased with decreasing alpha platelet thickness. At the strain rate of 10^{-4}/sec, the same trend was observed for the microstructures of '4μm' and '8μm', but the peak stress for the microstructure with the thinnest alpha ('1μm') exhibited the lowest peak stress. Considering that thin lamellar material is generally stronger than that of thicker one, it is unusual behavior.

This anomalous behavior is corresponding to the results obtained from load-relaxation test and compression test [7]. Two possible mechanisms that may explain this anomalous behavior are the change of slip system at low strain rate and the influence of thermally activated process such as diffusion. To clarify this problem, room temperature tensile tests were carried out using initial strain rate of 10^{-4}/sec. Before the tests, the specimens were held at 815°C for 30 min and quenched to exclude possible effect of phase volume fraction. As shown in Fig. 14(c), the anomalous behavior was not occurred at room temperature tensile tests. This result means that the changes in order of flow stress at low strain rate is resulted from the thermally activated process. In creep test condition, total deformation may depend on diffusion process rather than dislocation glide. The test condition used in this test is 815°C and 10^{-4}/sec which is similar to that of creep test. Thus, thin alpha plate material which have much larger diffusion path such as grain boundary can deform more
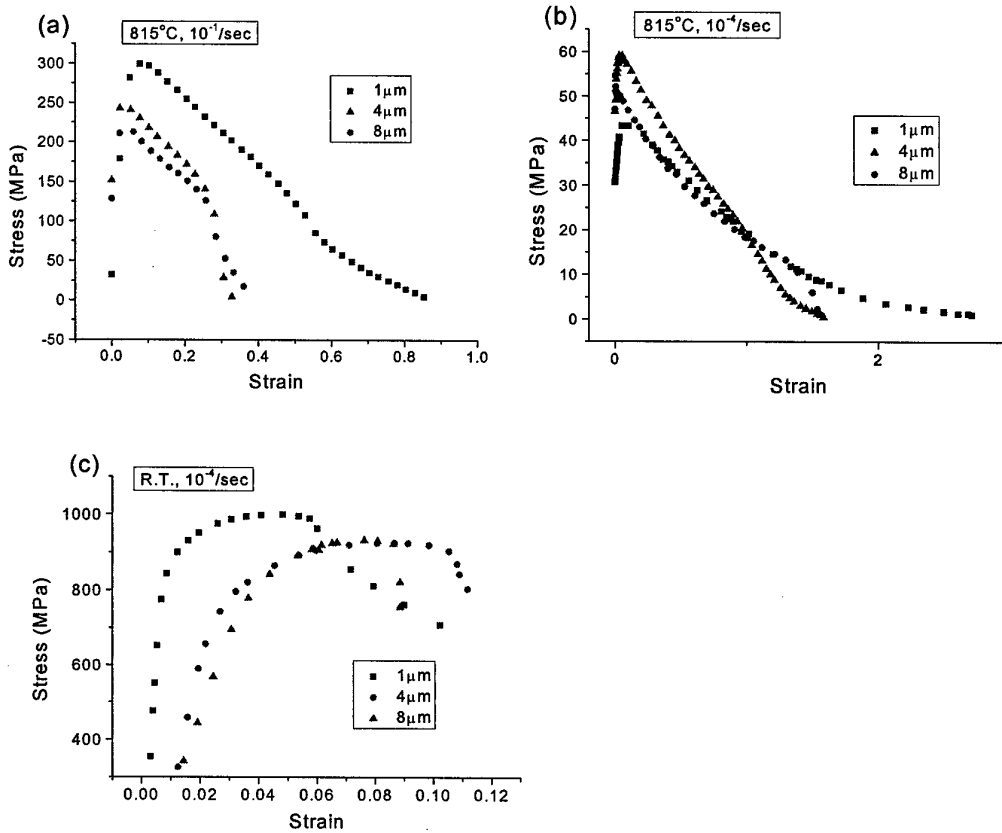
easily at lower flow stress.

Fig.14. Flow stress-strain curves obtained from tensile tests at 815°C using initial strain

rate of; (a) 10^{-1}/sec and (b) 10^{-4}/sec ; and (c) at room temperature, 10^{-4}/sec.

Fig. 15 shows plots of log σ vs. reciprocal temperature obtained from load-relaxation

tests. The value of the slope, $S = [\partial \log\sigma / \partial(1/T)]_{\dot{\varepsilon} \varepsilon}$, for the linear plots in Fig.15, is about

6038K at a strain rate of 10^{-4}/sec. An apparent activation energy, Q, can be calculated as

Q= 2.303 RS/m [22], where R and m are the universal gas constant and strain rate

sensitivity, respectively. Using the average values of $m \cong 0.35$ and S=6038K obtained at

815°C and 10^{-4}/sec, Q is computed as 290 kJ/mole. This value is quite different from the

activation energy of boundary diffusion in α-Ti (101 kJ/mole [23]), but similar to that of V

in β-Ti (240 kJ/mole [24]). This result supports that changes in the order of flow stress at low strain rate is presumably due to diffusion process of V in β-phase. However, it cannot necessarily be concluded that this is the rate controlling step since the presence of Al would have an affect on the V diffusion rate and vice versa [25].
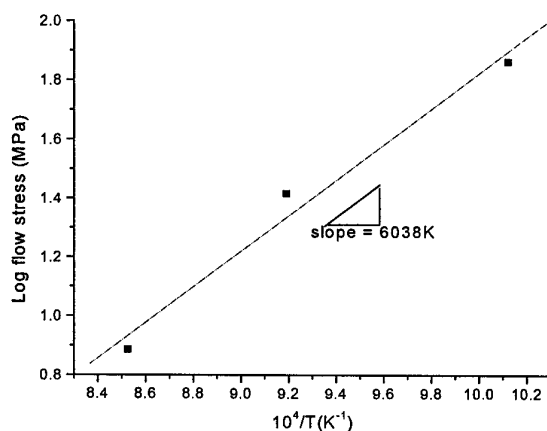

Fig.15 Variation of the flow stress obtained from load-relaxation tests with the reciprocal temperature at a strain rate of 10^{-4}/sec.

6. Conclusion

High temperature deformation mechanisms of Ti-6Al-4V alloy with a transformed microstructure were investigated in view of internal variable theory of inelastic deformation. The following conclusions were drawn from this investigation.

1. A series of load-relaxation tests were conducted on microstructures containing various alpha platelet thicknesses ranging from approximately 1 to 8 μm at 900°C. With decreasing alpha platelet thickness, flow stress increased at higher strain rates (i.e. $\dot{\varepsilon} \geq 10^{-2}$), but the trend was reversed at lower strain rates (i.e. $\dot{\varepsilon} \leq 10^{-3}$) presumably due to diffusion process of

V in β-phase

2. The flow stress-strain rate curves obtained by load relaxation tests at 715°C~900°C ($\varepsilon \approx$ 0.05) were well described by the equation for grain matrix deformation. However, for the heavily deformed ($\varepsilon \approx 1.2$) specimen, the flow stress-strain rate curves changed its shape at the intermediate strain rate region. It was attributed to the operation of grain boundary sliding, the rate of which was highest in the microstructure with the thinnest alpha laths/platelets.

3. Degree of flow softening at the strain rate of 10^{-1}/sec was largest in the finest lamellar microstructure because grain boundary area increased most rapidly due to dynamic globularization above equicohesive temperature. Flow softening behavior was closely related to the decrement of internal variable strength.

References

[1] Sellars, C.M. and Zhu, Q. *Materi. Sci. Eng. A*, , 2000, A280, pp. 1.

[2] D. Eylon and C.M. Pierce, *Metall. Mater. Trans. A*, 1976. vol. 7A, pp. 111-121.

[3] E.W. Collings, *The Physical Metallurgy of Titanium Alloys*, ASM, 1984, pp.39-45.

[4] R.C. Picu and A.Majorell, *Materials Science and Engineering A.*, A326, 2002, pp. 306.

[5] R.M. Miller, T.R. Bieler, and S.L. *Semiatin, Scripta Mater.* Vol. 40, No. 12, 1999, pp. 1387

[6] S.L. Semiatin and T.R. Bieler, *Metall. Mater. Trans. A*, 2001, 32A, pp. 1787.

[7] S.L. Semiatin and T.R. Bieler, *Acta Mater.*, vol. 49, 2001, pp. 3565.

[8] S.L. Semiatin, V. Seetharaman and I. Weiss, *Materials Science and Engineering A*, vol. A263, 1999. pp. 257-271.

[9] E.B. Shell and S.L. Semiatin, *Metall. Mater. Trans. A*, vol. 30A, 1999, pp. 3219.

[10] S.L. Semiatin, P.A. Kobryn, E.D. Roush, D.U. Furrer, T.E. Howson, R.R. Boyer and D.J. Chellman, *Metall. Mater. Trans. A*, vol. 32A, 2001, pp. 1801.

[11] T.R. Bieler, S.L. Semiatin, *Inter. J. of Plasticity*, 2002, vol. 18, pp. 1165-1189.

[12] T.K. Ha and Y.W. Chang, *Acta Mater*, vol. 46, 1998, pp. 2741.

[13] T.K. Ha, Y.N. Kwon and Y.W. Chang, *Mat. Sci. Forum*, vol. 217-222, 1996, pp. 1203.

[14] J.S. Kim, Y.W. Chang and C.S. Lee, *Metall. Trans. A*, vol. 29A, 1998, pp. 217-226

[15] J.H. Kim, D.H. Shin, S.L. Semiatin and C.S. Lee, *Materials Science and Engineering A*. A344, 2003, pp. 146.

[16] D. Lee and E.W. Hart: *Metall. Trans.*, 1971, vol. 106, pp. 1245.

[17] I. Weiss, F.H. Froes, and D.Eylon, and G.E. Welsch, *Metall. Trans. A*, vol. 17, 1986, pp. 1935.

[18] H.J. Jun, *MS dissertation*, POSTECH, 2000

[19] K.A. Lee, *Ph.D dissertation*, POSTECH, 1999

[20] J.W. Edingtion, K.N. Melton, and C.P. Cutler, *Progress in Mater. Sci.* 1976, 21, pp. 63-170.

[21] D.A. Holtm W.A.Backofen, Teans. Am. Soc. Met. 1966, vol. 59, pp. 755.

[22] V. Seetharaman and S.L. Semiatin, *Metall. Trans. A*, vol. 28, 1997, pp. 2309.

[23] C.H. Hamilton, A.K. Gosh, and M.W. Mahoney, Advanced Processing Methods for Titanium Alloys (edited by D.F. Hasson and C.H. Hamilton), TMS-AIME, Warrendale, Pa (1982), pp. 129-144.

[24] J.F. Murdock, T.S. Lundy, and E.E. Stansbury, *Acta metal.*, 1964, vol. 12, pp. 1033

[25] C.H. Johnson, S.K. Richter, C.H. Hamilton, J.J. Hoyt, *Acta Mat.*, 1999, vol. 47, pp.23.

Chapter 4

Summary and Statement
of Future Work

1. Summary and Statement of Future Work

In the earlier work of Lee et al [1], which has been carried out recently, the constitutive equation consisting of grain matrix deformation (dislocation glide and dislocation climb) and grain boundary sliding (GBS) has successfully described the deformation behavior of transformed microstructures of Ti-6Al-4V alloy at high temperatures (715°C ~ 900°C). However, for the heavily deformed specimen ($\varepsilon \approx 1.2$), additional deformation mechanism is observed to occur in the flow stress - strain rate curve, which is identified as grain boundary sliding by the microstructural analysis. They have also reported that the grain boundary sliding is more prevalent in thin alpha material since thin alpha platelet material is more easily globularized than thick alpha material. Flow softening of heavily deformed material has been attributed to the decrease of internal strength variable (σ^*) due to globularization and the occurrence of grain boundary sliding.

Although the high temperature deformation behavior of Ti-6Al-4V alloy with lamellar type microstructure has well been analyzed by the inelastic deformation theory, several important aspects are not clarified yet, and need to be investigated.
They are summarized as follows.
1. Changes in the order of flow stress at low strain rate.
2. Morphological effect on dislocation permeability parameter.
3. Evidence of dislocation climb.
4. Flow softening at different strain level.
5. Deformation mechanisms of ultra-fine grained material.

Therefore, this investigation aims to clarify the above mentioned points.

2. Objectives

The objectives of future research work are classified into three main categories.

(1) <u>Detailed Analysis on flow stress – strain rate curves (Supplementary of 1st year work)</u>
- Quantification of each deformation process (dislocation slip, dislocation climb and grain boundary sliding) in the flow stress-strain rate curve at specified temperature and stress.
- Why the order of flow stress changes at low strain rate? Is it due to morphological effect? Or due to the activation of new mechanism?
- Deeper analysis on dislocation permeability parameter (p): why p=0.1?
- Flow softening at different strain level: load relaxation test after $\varepsilon \approx 0.6$.
- Load relaxation test by compression

(2) <u>Microstructural Analysis (Supplementary of 1st year work)</u>
- Experimental measurement of grain boundary sliding (and grain matrix deformation by indirect method)- compare the result with (1)
- Evidence of dislocation climb: - investigation of sub-grain boundaries by TEM
- The place of recrystalization: - α/α. β/β or α/β boundary?

(3) <u>Investigation on deformation mechanisms of ultra-fine grained material</u>
- Constitutive analysis on the high temperature deformation of ultra-fine grained

material
- Any difference in the flow stress- strain rate curve (or any new mechanism?) as compared with those of 8μm and 1μm microstructures?

3. Experimental Details

3. 1. Materials and Heat Treatments

This year's experimental scheme will be the same as last year using microstructures with different lamellar spacings; (a) fine (≅ 1μm), (b) intermediate (≅ 4μm), and (c) coarse (≅ 8μm) lamellar spacing, respectively. Each of these microstructures is then subsequently preheated at 715, 815 and 900°C for 15 min. for load relaxation tests,

To investigate the *contribution of dislocation glide and dislocation climb quantitatively*, *single-phase alpha alloy* having the same composition as the alpha in the two-phase alloy Ti-64 will also be used in this study.

3. 2. Load Relaxation Tests

Load relaxation tests will be carried out to evaluate the flow stress characteristics of transformed microstructures with different lamellar spacings. The tests will be carried out in Ar atmosphere at three different temperatures; 715, 815, and 900°C. Round specimens with a gauge diameter of 6mm and a gauge length of 15mm will be used for the tests. The flow stress and inelastic strain rates obtained by load relaxation tests will be analyzed by a non-linear regression method of commercial curve fit program. Also, the results transformed microstructures of will be compared and discussed with those of equiaxed microstructures [2,3].

Last year, the tests have been performed only for the specimens imposed by a small amount of strain ($\varepsilon = 0.04$) and a large amount of strain ($\varepsilon = 1.2$) This year, *specimens imposed by an intermediate strain ($\varepsilon = 0.6$) will be tested.* The results will manifest the critical strain to induce recrystallization.

Load relaxation test in compression has never been reported so far. That is probably due to the fact that the end effect (due to the friction between the die and the specimen) is so large that it will be difficult to interpret load relaxation data by compression tests. However, we will attempt to do load relaxation test in compression and compare the data with those in tension.

3. 3. Constitutive Analysis

As mentioned in the objectives, our main efforts will be given to investigate high temperature deformation mechanisms *in a quantitative manner by performing thorough constitutive analysis* of flow stress and strain rate curves.

3. 4. Optical and TEM Microscopy

Microstructures before and after the deformation will be analyzed by both optical and transmission electron microscopy. Special attention will be paid to investigate *the place of recrystalization and the evidence of dislocation climb* by transmission electron microscopy.

4. References

1. J.H. Kim, S.L. Semiatin and C.S. Lee, *Mat. Sci. Forum*, accepted, 2003.
2. J.S. Kim, J.H. Kim, Y.T. Lee, C.G. Park and C.S. Lee, *Materials Science and Engineering A*, Vol. A263, 1999, pp. 272-280.
3. C.S. Lee, S.B. Lee, J.S. Kim and Y.W. Chang, *International Journal of Mechanical Sciences*, Vol. 42, 2000, pp. 1555-1569